Received: 4 January 2024 | Accepted: 5 March 2024

DOI: 10.1111/1365-2745.14306

Journal of Ecology BRITISH ECOLOGICAL SOCIETY

RESEARCH ARTICLE

Precipitation seasonality and soil texture interact to shape dryland recovery from severe disturbance

Tyson J. Terry[1,2] | **Peter B. Adler**[2]

[1]Department of Disturbance Ecology, Bayreuth University, Bayreuth, Germany

[2]Department of Wildland Resources and the Ecology Center, Utah State University, Logan, Utah, USA

Correspondence
Tyson J. Terry
Email: tysonjterry@gmail.com

Funding information
Strategic Environmental Research and Development Program, Grant/Award Number: 201940; Utah State University, Grant/Award Number: A07339-1068

Handling Editor: Yann Hautier

Abstract

1. Disturbances drive large changes in plant composition and ecosystem functioning in drylands, but current understanding of how recovery following disturbance depends on the environment is limited due to challenges in analysing effects of disparate disturbances across abiotic gradients.
2. We combined remote sensing and field observations across 5600+ km of natural gas pipeline corridors and adjacent undisturbed vegetation to investigate how recovery from a uniform, severe disturbance varied with factors that influence water availability in drylands.
3. We found that recovery of net primary production (NPP) often remains incomplete, with only 42% of our sites projected to fully recover within 100 years. NPP recovery was quicker and more complete in regions that receive most of their annual precipitation at low temperatures and have fine-textured soil; recovery of total shrub cover (median timing of 81 years) was faster on fine-textured soils in locations that receive most of their annual precipitation at high temperatures. Locations with quick recovery of shrub cover were linked with a shift in dominant shrub species and incomplete NPP recovery.
4. *Synthesis*. Recovery of NPP and shrub cover in drylands were driven by different environmental factors. For both NPP and shrub cover, locations with high pre-disturbance values required more time to recover to adjacent undisturbed levels than locations with low pre-disturbance values. Quick recovery of shrub cover or productivity was generally linked with a shift in dominant plant species or functional group.

KEYWORDS
desert, disturbance, net primary production, plant–climate interactions, precipitation timing, recovery, resilience, shrub, soil texture

1 | INTRODUCTION

Ecological disturbances, natural or anthropogenic, cause long-lasting changes to vegetation in dryland systems (Allred et al., 2015; Boyd & Davies, 2012) and have been linked to shifts in stable states (Abella et al., 2021). Understanding recovery trajectories following disturbance is necessary for guiding management and conservation of lands that are susceptible to long-term impacts

(Chambers et al., 2017). However, great uncertainty exists concerning recovery rates and how they depend on environmental factors in drylands (Stafford Smith et al., 2009). This uncertainty reflects the short-term nature or limited spatial scale of previous disturbance studies (O'Brien et al., 2022).

The lack of spatially extensive disturbance studies in drylands stems from multiple challenges that make it difficult to compare impacts of different disturbances occurring in separate locations. Disturbances vary in type, severity, timing and patchiness, all of which influence post-disturbance dynamics and complicate spatial comparisons (Bartels et al., 2016; Díaz-Delgado et al., 2003). Furthermore, vegetation types characterized by different disturbance regimes usually have different climates. Funding generally limits the spatial and temporal scale of recovery monitoring such that disturbance data is often post hoc, comprised of many space-for-time substitutions that may not capture long-term recovery pathways. Many studies compare the value of a response variable after the disturbance to a pre-disturbance baseline, but this approach may also be unreliable because it assumes a steady-state equilibrium that is unlikely in an era of changing climate and invasive species (Monroe et al., 2022; Parker & Wiens, 2005).

Recovery, which we define as the return of a variable to its undisturbed state following a perturbation (Chambers et al., 2019; Oliver et al., 2015), comprises two processes: the initial, short-term response of a variable to the disturbance and subsequent changes over time following the initial response (Hodgson et al., 2015; Ingrisch & Bahn, 2018). These two processes are comparable to resistance (degree of initial response) and engineering resilience (rate of recovery after initial response) (Ingrisch & Bahn, 2018; Nimmo et al., 2015).

A common hypothesis is that the rate of recovery of plant communities following a disturbance depends on resource availability (Chapin et al., 1996; Shriver et al., 2018; Tilman, 2016). In drylands, water availability is the key resource driving net primary production (NPP) and vegetation dynamics (Chambers et al., 2014; Jordan et al., 2020), with previous studies showing that wetter areas or weather periods promote recruitment success (Nelson et al., 2014; O'Connor et al., 2020). However, recovery of a system following disturbance requires a return to current undisturbed levels of function and structure (Chambers et al., 2019; Oliver et al., 2015), and many of the studies supporting this hypothesis in drylands do not compare post-disturbance growth with contemporary undisturbed controls.

An alternative hypothesis we propose, is that recovery in drylands may be faster in low-resource environments with sparse vegetation. For example, dry areas might recover more quickly than wet areas due to the small amount of growth needed to recover to the relatively low level of productivity found in dry undisturbed control sites, whereas wetter areas may require substantially more time to recover the comparatively high levels of productivity found in wetter undisturbed sites. This relative-recovery hypothesis emphasizes the importance of undisturbed reference conditions to quantify recovery. Moreover, including undisturbed controls becomes necessary to compare recovery across climatic gradients (Parker & Wiens, 2005), especially in drylands where primary production potential and species composition are strongly tied to water availability (Sala et al., 2012).

Recovery from disturbance often depends on recruitment, which in drylands is tightly linked with soil water availability (Bradford et al., 2019; Nelson et al., 2014). Water availability in drylands is largely determined by interactions between precipitation quantity, seasonality and soil texture (Loik et al., 2004; Renne et al., 2019). Coarse soil texture may benefit deep-rooted plants in arid conditions, where high infiltration reduces loss of soil water to evaporation and increases water availability in deep soil layers (Maurer et al., 2020; Noy-Meir, 1973; Walter, 1964). However, the benefits of coarse soil texture decline with increases in total precipitation, as losses of soil water to deep drainage outweigh the benefits of low evaporative losses (Noy-Meir, 1973). This idea, commonly known as the inverse texture hypothesis, is largely supported by studies of NPP (Sala et al., 1988) and mature plant abundance (Renne et al., 2019). However, the effect of coarse soils on recruitment remains unclear for shallow-rooted seedlings (Barnard et al., 2019; Boyd & Davies, 2012). Seasonal timing of precipitation also impacts evaporative losses (Lauenroth & Bradford, 2012) that are thought to determine the benefits of coarse soil texture for plant growth (Renne et al., 2019). Testing hypotheses about water availability and recovery following disturbance in drylands therefore requires careful consideration of interactions between seasonal precipitation regimes and soil properties.

Natural gas pipeline corridors provide an opportunity to investigate variation in recovery across environmental gradients, overcoming common limitations of traditional disturbance studies. Pipeline corridors create a near-uniform pulse disturbance that runs hundreds of kilometres, spanning broad soil and climate gradients. Pipeline installation consists of removing all above-ground biomass via bulldozer in a strip we refer to as the corridor (up to 35 m wide), followed by digging a trench and burying a 20- to 30-cm-diameter pipe down the centre of the cleared corridor. This disturbance not only removes all plants but also displaces and compacts surface soil (Shi et al., 2014). Following construction, topsoils are spread back over the corridor and then seeded for restoration. Post-construction seeding efforts generally use seed mixes to match native species and functional types, but these efforts are often unsuccessful and with mixed effects on species composition (Farrell & Fehmi, 2018; Rottler et al., 2018). Construction effects are largely concentrated within the pipeline corridors, leaving undisturbed neighbouring vegetation and soils as a control to measure recovery. Instead of relying on historical, pre-disturbance conditions as the baseline for measuring recovery, this data set allows yearly comparisons of disturbed and undisturbed vegetation to account for changes over time in undisturbed sites.

Here, we studied two dimensions of ecosystem recovery following pipeline disturbance: total shrub cover and NPP. Shrub cover represents a dominant plant functional type in North American drylands (Peinado et al., 1995), where many imperilled wildlife species are considered shrub obligates (Suring et al., 2005). NPP represents the rate at which energy enters the ecosystem and is an indicator of dryland degradation (Wessels et al., 2008; Zika & Erb, 2009). We used annual remotely sensed estimates of NPP and total shrub cover along natural gas pipeline corridors to answer two research questions: (1) How long does it take for NPP and shrub cover in drylands to recover following a disturbance that removes all biomass and disrupts the surface soil? (2) How do mean annual precipitation (MAP), precipitation seasonality and soil texture interact to influence time to recovery of NPP and shrub cover in drylands? We hypothesized that interactions between climate and soils that increase water availability could either (a) increase recruitment and speed up recovery of both NPP and shrub cover, or (b) create high undisturbed values of NPP and shrub cover that require more time to recover.

2 | METHODS

2.1 | Pipelines

We used The National Pipeline Mapping System (USDOT, 2021) to identify pipelines within the Great Basin, Mojave, Chihuahuan and Sonoran deserts. We selected wide (25+ m) and long (>300 km) pipelines to allow use of high-resolution satellite imagery products derived from Landsat satellites and to span broad, spatial environmental gradients within and among desert systems. Our data came from four natural gas pipeline corridors: Kern River Pipeline (2702 km, built in 1992), Ruby Pipeline (1090 km, built in 2011), El Paso Natural Gas Pipeline (1040 km, built in 1946) and Northwestern Pipeline (860 km, built in 1960). We determined date of construction (initial disturbance) as the midpoint date between the start and completion of construction, a process of 1–2 years. We also contacted pipeline company restoration specialists to confirm there were no additional large-scale disturbances such as herbicide application, new pipelines in the same corridor or additional large-scale removal of biomass. Other historic disturbances such as grazing and/or wildfire were not accounted for; we assume they have equal effect on disturbed and undisturbed pixels due to their proximity.

We used annual remotely sensed metrics from the period 1986–2019 and combined pipelines with differing initial construction dates to quantify recovery up to 73 years since disturbance (YSD) (Figure 1). To define the centre of pipeline corridors, we manually drew spatial reference lines within Google Earth Engine (Gorelick et al., 2017) using their high-resolution satellite basemap (<1 m resolution) while also consulting maps from The National Pipeline Mapping System (USDOT, 2021). We selected Landsat pixels (30 m resolution) that fit within these pipeline corridors by only using pixels whose centroid was within 3 m of the reference lines. This allows a maximum of 11% of a pixel to fall outside the pipeline corridor, depending on pixel orientation and position. For undisturbed controls, we used the nearest neighbour along an undisturbed line adjacent to the pipeline corridor. We manually drew the undisturbed comparison lines parallel and near the pipeline corridor (average distance of 120 m from pipeline corridor). Undisturbed comparison lines were visually inspected with elevational raster data sets and high-resolution imagery to ensure they represented similar topography and land use as the pipeline corridor. Locations where the pipeline corridor or comparison line differed in topography or land use were excluded

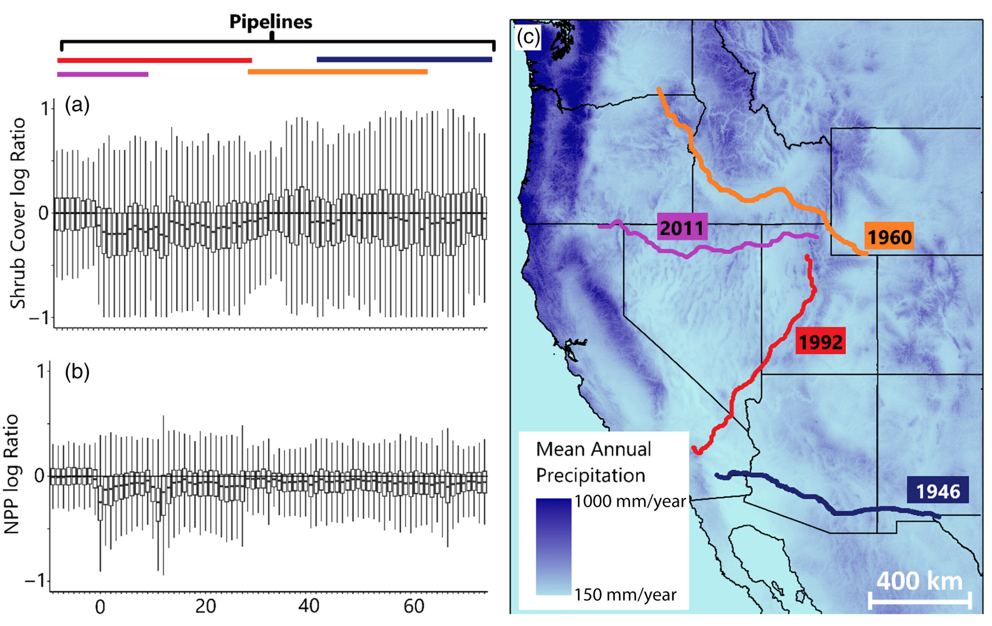

FIGURE 1 Shrub cover and net primary production (NPP) ratios before and after pipeline disturbances and pipeline locations. (a) Shrub cover from remotely sensed data in log-ratio form of shrub cover recovery (value of 0 indicates equal shrub cover on disturbed pipeline pixel and undisturbed control pixel) with colours indicating the different pipelines used in the study. (b) Remotely sensed values of NPP in ratio form (disturbed pipeline corridor value/undisturbed control value). (c) Pipeline corridor locations and the year of construction for each respective pipeline. Boxplots in (a, b) represent the median (centre mark), the 25th and 75th percentiles (upper and lower limits of box) and the additional variance of non-outlier data beyond those percentiles (lines extending from boxes).

from the data set. Both our disturbed and undisturbed reference lines exclude croplands, roads and urban areas. To quantify recovery, we divide the NPP or shrub cover in each individual pipeline pixel by the corresponding value in the nearest undisturbed neighbour pixel. This ratio represents the recovery of the pipeline pixel relative to the nearest undisturbed pixel in the same year. Altogether, our data set includes 18,239 pairs of disturbed and undisturbed pixels.

2.2 | Remote sensing data

We used a publicly available data set to estimate NPP across time and space (Robinson et al., 2019). This product utilizes reflectance values from Landsat imagery (30-m resolution) and cover estimates from an annual plant functional cover data set (Jones et al., 2018) to estimate annual NPP. The NPP algorithm accounts for within-pixel heterogeneity of plant functional types, and adjusts for changes in vegetation type that may occur following disturbance. We used estimates of total annual NPP from this data set by combining the NPP estimates from all plant functional groups. NPP data specifically represent net carbon uptake (in grams per square metre) on a yearly basis.

We used the Rangeland Analysis Platform data set (version 2.0) for annual estimates of plant cover (Allred et al., 2021). The data set uses a temporal convolutional neural network to estimate annual per cent cover of the following plant functional groups: annual forbs and grasses, perennial forbs and grasses, shrubs, trees and bare ground. This data set utilizes both temporal and spatial smoothing to produce a continuous data set despite gaps in imagery time-series caused by cloud cover. The algorithm predicted shrub cover with an R^2 of 0.57 and a mean absolute error of 5.8 on an independent validation data set (Allred et al., 2021).

MAP was derived from a gridded climate product, Daymet (Thornton et al., 2022). Daymet produces gridded surfaces (1000 m^2 spatial resolution) of daily weather parameters based on daily meteorological observations. Annual precipitation values were calculated for each water year (October 1–September 30) to understand how water inputs relevant to each growing season are impacting recovery. Soil texture data (percent sand content) represent an arithmetic average value of soil texture estimates of the top 30 cm obtained from OpenLandMap (250-m resolution) (Tomislav, 2018), with methods described in Hengl et al. (2017). Our metric of precipitation seasonality was mean temperature of wettest quarter (MTWQ; 1-km resolution) (Fick & Hijmans, 2017).

2.3 | Data cleaning

The continuous nature of pipeline corridors and mountainous terrain led to incorporation of many pixels that do not fall within our focus on dryland vegetation. As a result, before initial analysis, we removed all pixels with >20% tree cover and >600 mm of rainfall. Due to the sensitivity of our recovery ratio metric to zeros and extremely small values, we also removed pixels from barren locations with extremely low 30-year mean annual NPP values (<10 g C/m^2), and all pixel-years with values of zero. For quality control of remote sensing products, we excluded pixels with >15% temporal gaps caused by missing data and/or cloud cover in their annual Landsat imagery composites.

2.4 | Field surveys

The purpose of these surveys was to provide a qualitative comparison of remote sensing data to field survey data. We also sought to determine whether shrubs recovering after the disturbance belonged to the same dominant shrub species as undisturbed controls and whether that varied across space, which we could not deduce from our remotely sensed plant functional group data.

We conducted field surveys at a total of 49 sites across the four pipelines during the years 2021–2022 (Figure S7). We specifically selected sites to represent the range of annual precipitation across each pipeline. Field observations were made during peak green-up for each system: mid-April 2022 for the Mojave Desert sites, mid-September 2021 for the Chihuahuan desert sites and late-May 2021 for the Great Basin sites. At each site, we completed four total transects: two parallel 30-m transects within the disturbed pipeline corridor and two parallel 30-m transects in undisturbed vegetation 50 m adjacent to the pipeline corridor. We used a line transect technique to measure percent canopy cover of individual plant taxa. We identified all shrubs to species and all other taxa to species or genus. For small plants (canopy diameter less than 100 cm), we classified cover as canopy gaps less than 5 cm. For large plants (canopy diameter greater than 100 cm), we classified cover as canopy gaps less than 10 cm.

2.5 | Statistical approach

Our modelling approach assumes that the pulse disturbance of pipeline construction has an initial impact on NPP and shrub cover, which is followed by more gradual changes over time in the subsequent YSD (see equation in Figure 2). We quantified recovery, our response variable, as the ratio of disturbed to undisturbed values for annual NPP and shrub cover (remotely sensed) (Figure 2). With this ratio approach (Avirmed et al., 2015), a value of ~1, or 0 on the log scale, indicates identical values of a variable in the disturbed and undisturbed pixels. We log-transformed the ratio to normalize the asymmetrical shifts in ratio values that accompany changes in the numerator and denominator values (Isles, 2020). Model predictions were back-transformed to arithmetic scale for ease of interpretation. Pre-disturbance data are a ratio of pixels that are located in the path of the future pipeline corridor (prior to construction) and neighbouring pixels outside the path of the future pipeline corridor.

We used a mixed effects linear model in the lme4 package in R (Bates et al., 2015; R Core Team, 2022) that assumed the recovery ratio is explained by factors that modify water availability: MAP

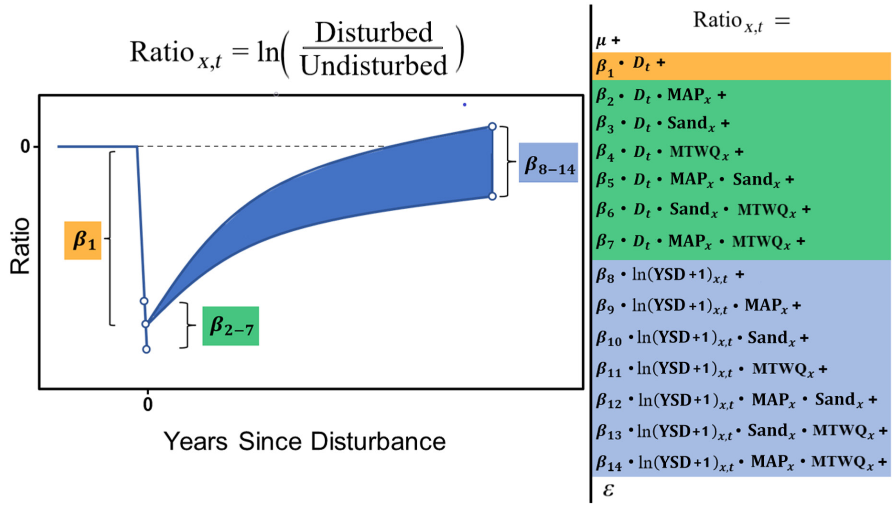

FIGURE 2 Statistical model visualized to show how covariates can shape initial impact (*D*) and recovery trajectory (ln(YSD + 1)). The yellow colour coding indicates the initial impact of disturbance (*D*). Green colour coding indicates how environmental factors of mean annual precipitation (MAP), soil sand content (Sand), mean temperature of wettest quarter (MTWQ), and their interactions influence the initial impacts of disturbance (*D*). Blue colour coding indicates time since disturbance (ln(YSD + 1)) and how environmental factors of MAP, Sand, MTWQ and their interactions shape long-term recovery. The random effects of pipeline company interacting with both *D* and ln(YSD + 1) are not shown in the formula but were included in our models. YSD term indicates years since disturbance.

(Condon et al., 2011), MTWQ (Nelson et al., 2014), per cent soil sand content (Sand; Germino et al., 2018; Maurer et al., 2020; Renne et al., 2019) and their respective two- and three-way interactions. Each of these environmental covariates varies spatially among pixels (x). We also included a binary disturbance variable, D, with values of 1 (disturbed) or 0 (undisturbed), as well as a variable allowing recovery following disturbance ($\ln(YSD_{x,t}+1)$), which varies across pixels (x) and years (t) (equation in Figure 2). This time since disturbance variable, ($\ln(YSD_{x,t}+1)$), was calculated at all disturbed pixels, with 1 being added to the YSD such that for the year of pipeline completion (YSD = 0), the value would equal 0. As shown in Figure 2, this model allows MAP, MTWQ, Sand and their interactions to influence the recovery ratio by interacting with the initial impacts of disturbance (D) and YSD ($\ln(YSD_{x,t}+1)$). We performed various simulations with different potential recovery trajectories and found that using this disturbance metric allowed for a flexible model that did not allow initial disturbance values to bias long-term recovery dynamics.

To account for variation in restoration efforts and differing widths of corridors that result from different pipeline companies, we included pipeline identity (e.g., Kern River pipeline) as a random effect on both initial disturbance impact and recovery rate. To account for spatial autocorrelation in our remotely sensed data, we utilized a modified spatial block bootstrap approach (Zhu & Morgan, 2004), where we took random stratified subsamples of our data set using spatial covariates of MAP and soil sand content as criteria. This approach limits similarity in spatial attributes that occur when pixels occur closely in space but retains a large range of environmental values to inform the interaction terms within our model. We fit our linear mixed effects model on each stratified bootstrap subsample of the data (~1300 sites/pixels) that comprised 7% of the data set and included all years of data for those selected sites (~37,000 site/pixel-years). We then calculated the median coefficient estimates from 1000 bootstrap iterations and their respective 95% confidence intervals. We considered effects to be statistically significant if the 95% confidence intervals did not overlap with zero. For interpretation purposes and to account for observation error, we quantified full recovery as a return to within 95% of undisturbed levels. Model fit was assessed by checking diagnostic plots to ensure no trends between residuals and fitted values and that residuals had a normal gaussian distribution (Figures S1 and S2).

We created a separate linear regression model to analyse our field data and determine whether the shrub species that grows following disturbance matched the dominant shrub species found in undisturbed neighbouring vegetation. The response variable was the ratio of dominant shrub species cover, with the cover (%) of the most abundant shrub species in the undisturbed transects as the denominator and the cover (%) of that same species within the disturbed pipeline corridor as the numerator. Explanatory variables were temperature of wettest quarter (described below) and YSD, and we did not include random effects.

2.6 | Precipitation regimes

Our models used the variable 'mean temperature of wettest quarter' to represent differences in the vulnerability of precipitation to evaporative demand. To facilitate interpretation and visualization of model results and predictions, we divided the study region into three categorical precipitation regimes based on the temperature of the wettest quarter (Figure S3). These regions represent areas that receive the majority of their annual precipitation (water year October–September) in cold (<4.5°C), cool (4.5–17°C) and warm temperatures

Journal of Ecology BRITISH ECOLOGICAL SOCIETY

(>17°C). Cut-off points for separating these three desert types were determined visually by natural breaks in the distribution of the temperature of the wettest quarter (Figure S3). More traditional classifications divide deserts into warm deserts (majority of precipitation received during summer) and cold deserts (majority of precipitation received during winter), but the temperature of the wettest quarter provides more information about evaporative demand when most precipitation falls, which was our primary interest. Additionally, we used quantile values of 33% and 66% of MAP in our data set to create cut-off values for three categories of MAP. We used these cut-offs for visualization purposes only; they played no role in model fitting. We chose visualization cut-offs for fine versus coarse soil texture using quantile values of 40% and 60% of soil sand content, respectively.

3 | RESULTS

3.1 | Model performance

NPP and shrub cover recovery varied dramatically in space and time in our remotely sensed data set (Figure 1). Average R^2 values after 1000 bootstrap iterations for our NPP and shrub cover models were 0.30 and 0.41, respectively (conditional). The substantial unexplained variation in our data set indicates the importance of sources of variation not included in our model. Both the NPP and shrub cover models indicated significant relationships between our covariates and recovery, with large differences in variable importance between the two models (Table 1).

3.2 | Initial impacts on NPP

The initial impact of pipeline disturbance decreased annual NPP 11% on average. Sites with coarse soil were more negatively impacted, whereas areas with warmer precipitation regimes were less negatively impacted (Table 1; Figure 3). Interactive effects of MAP and precipitation seasonality on initial impacts were large but variable (Table 1).

3.3 | Long-term recovery of NPP

The long-term value of NPP was largely determined by the initial drop in NPP at the time of disturbance because little recovery occurred except in cold precipitation regimes with fine soils (Figure 3a). Recovery rate following initial disturbance impacts generally decreased with warmer precipitation regimes and higher annual precipitation (Figure 3). The interaction between Sand and MAP was the only interaction in our model that significantly affected recovery rate following initial disturbance (Table 1).

3.4 | Initial impacts on shrub cover

Total annual shrub cover was significantly impacted by the pipeline disturbance, dropping 23% on average. MAP, precipitation season and their interaction had the strongest effects on initial impacts of disturbance (Table 1). Areas that were wetter (higher MAP) and

TABLE 1 Coefficient estimates from bootstrapped linear model explaining recovery of shrub cover and net primary production (NPP). Lower and upper 95% values represent the 95% confidence interval of the coefficient estimate across 1000 bootstrap samples. Bolded values indicate values with confidence intervals that do not overlap zero and are interpreted as statistically significant. MAP is mean annual precipitation (mm/water year), Sand is % soil sand content, MTWQ is the mean temperature of the wettest quarter, *D* is a binary variable indicating whether a given data point is disturbed (1) or undisturbed (0), YSD is years since disturbance.

	Shrub cover			NPP		
Coefficient	Lower 95%	Median	Upper 95%	Lower 95%	Median	Upper 95%
Intercept	−0.039	**−0.036**	−0.025	0.026	**0.032**	0.047
D (disturbance)	−0.29	**−0.253**	−0.136	−0.146	**−0.116**	−0.008
D×MAP	0.101	**0.114**	0.154	−0.026	−0.01	0.045
D×Sand	−0.032	**−0.026**	−0.004	−0.06	**−0.053**	−0.027
D×MTWQ	0.094	**0.109**	0.167	0.013	**0.029**	0.084
D×MAP×MTWQ	−0.06	**−0.051**	−0.024	−0.023	−0.013	0.019
D×MAP×Sand	0.18	**0.197**	0.269	−0.004	0.019	0.098
D×Sand×MTWQ	−0.069	**−0.055**	−0.007	−0.006	0.009	0.062
ln(YSD+1)	0.044	**0.053**	0.084	−0.001	0.008	0.03
ln(YSD+1)×MTWQ	−0.041	**−0.037**	−0.025	−0.015	−0.011	0.003
ln(YSD+1)×Sand	−0.003	−0.001	0.007	−0.003	−0.001	0.007
ln(YSD+1)×MTWQ	−0.03	**−0.025**	−0.007	−0.022	−0.016	0.003
ln(YSD+1)×MAP×Sand	0.007	0.01	0.017	0.001	**0.003**	0.013
ln(YSD+1)×MAP×MTWQ	−0.053	**−0.047**	−0.031	−0.012	−0.007	0.014
ln(YSD+1)×Sand×MTWQ	0.002	**0.007**	0.021	−0.002	0.003	0.016

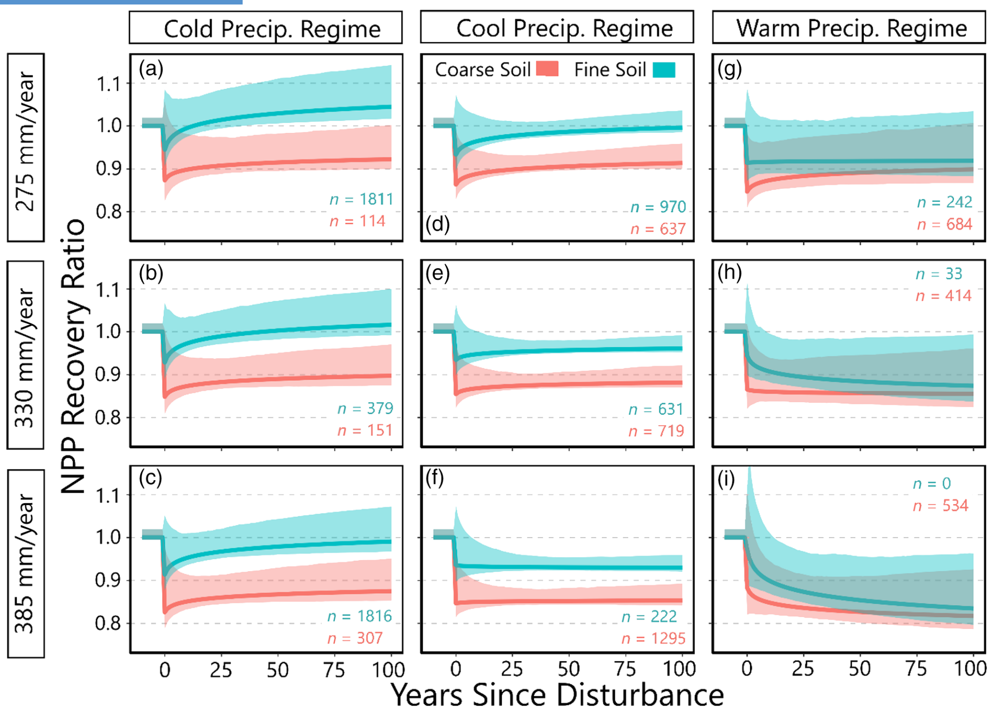

FIGURE 3 Predicted patterns of net primary production (NPP) recovery across North American deserts. The three columns represent spatial differences in precipitation timing: areas that receive a majority of their precipitation during periods of cold, cool and warm temperatures. The three rows represent different scenarios of mean annual precipitation. Colours represent coarse (40% soil sand content) and fine soil texture (30% soil sand content). Recovery values (*y*-axis) are a ratio of disturbed NPP (numerator) in relation to undisturbed NPP (denominator). A value of 1 indicates equal shrub cover on disturbed sites and undisturbed controls. *N* count values represent the number of corresponding sites within the dataset that match environmental conditions within each panel. Letter labels (a–i) are provided for more direct reference in the results and discussion sections.

belonged to warmer precipitation regimes had smaller initial negative impacts (Figure 4g–i). Effects of coarse soil texture (higher sand content) switched from slightly positive to negative when transitioning from cold to warm precipitation regimes (Figure 4; Table 1).

3.5 | Long-term recovery of shrub cover

Higher MAP and warmer precipitation season both significantly decreased the long-term shrub recovery rate (Table 1; Figure 4). Negative impacts of coarse soil on long-term recovery were stronger in warmer precipitation regimes (Figure 4g–i). A combination of high MAP and warm precipitation regime (not present in our data) shifted the recovery trajectory from initial-drop followed by positive recovery, into a trajectory of initial increase, followed by subsequent decline (Figure 4i).

3.6 | General recovery timelines

Across all our pipeline sites, our models predicted that 50% of sites will recover shrub cover within 81 years of disturbance, with 79% of sites recovering within 150 years (Figures S4 and S5), assuming recovery rates follow current trajectories. NPP recovery was predicted to occur rapidly (<20 YSD) at 40% of sites, with almost all other sites unlikely to recover within 150 years after the disturbance (Figures S4 and S5).

3.7 | Field observations

Field data showed that 52% of sites ($n=23$) at two old pipelines (61 and 75 YSD) had recovered total shrub cover to current undisturbed levels (Figure S6), agreeing well with our remotely sensed estimates of 53% recovery of all pipeline pixels for the same pipelines at that time post-disturbance. Average recovery ratio values based on field data across the same pipelines was 1.02, whereas the average of model estimates for the same pipelines was lower at 0.95.

Precipitation regime and YSD explained 38% of variance in dominant shrub recovery ratios across 49 field sites. Our field surveys indicate that shrub species composition following disturbance often differed from the dominant undisturbed shrub species and was significantly affected by MTWQ ($df=44$, t score $=-3.955$, $p<0.001$). Specifically, the similarity in shrub species composition between disturbed and undisturbed sites was highest in colder precipitation regimes (Figure S6).

4 | DISCUSSION

Current understanding of recovery following disturbance has been limited by the spatiotemporal scope of previous studies and complications such as variation in the type, timing and intensity of disturbance events across different plant communities. Our comparison

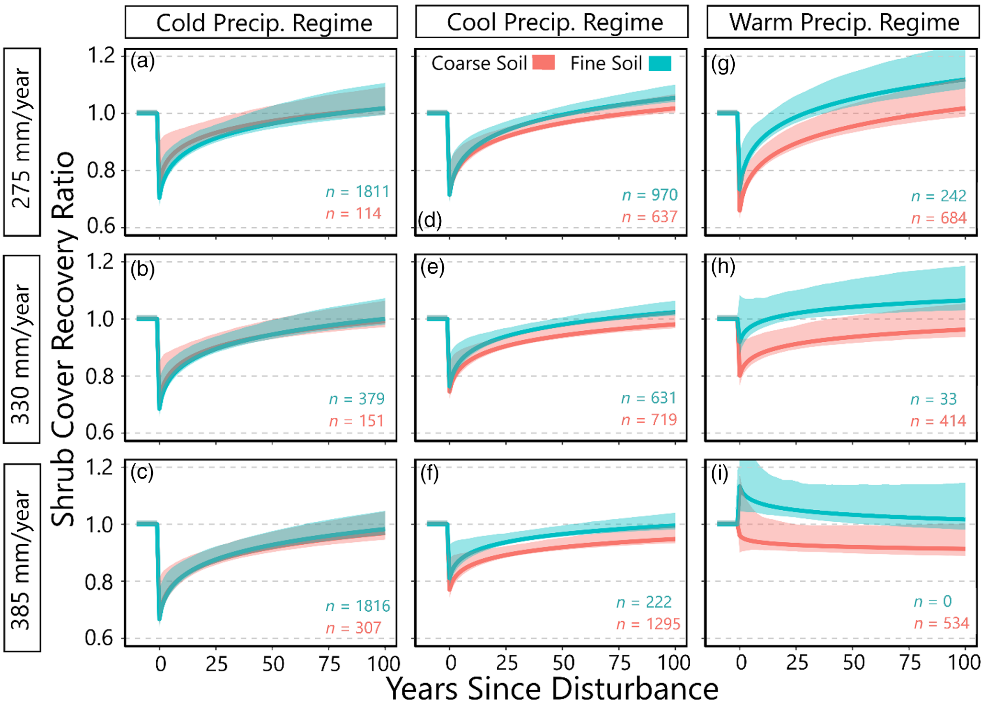

FIGURE 4 Predicted patterns of shrub cover recovery across North American deserts. The three columns represent spatial differences in precipitation timing: areas that receive a majority of their precipitation during periods of cold, cool and warm temperatures. The three rows represent different scenarios of mean annual precipitation. Colours represent coarse (40% soil sand content) and fine soil texture (30% soil sand content). Recovery values (*y*-axis) are a ratio of disturbed shrub cover (numerator) in relation to undisturbed shrub cover (denominator). With this system, a value of 1 indicates equal shrub cover on disturbed sites and undisturbed controls. Margins represent 95% confidence intervals from 1000 bootstrap model iterations. *N* count values represent the number of corresponding sites within the dataset that match environmental conditions within each panel. Letter labels (a–i) are provided for more direct reference in the results and discussion sections.

between disturbed and adjacent undisturbed vegetation across spatially extensive pipeline disturbances allowed us to investigate how recovery varied across environmental gradients that influence water availability. Though not representative of any natural disturbance, data from pipeline corridors enabled us to examine recovery across space following a uniform disturbance that removed vegetation and disrupted the surface soil.

We found that the initial impacts of disturbance and the rate of recovery following disturbance vary greatly across time and space (Figures 3 and 4). NPP and shrub cover did not recover simultaneously, but rather showed opposite patterns in recovery. Disturbance impacts to NPP were not large, but only 42% of sites were projected to recover to undisturbed production NPP levels within 100 years of disturbance (Figures S4 and S5). In contrast, disturbance impacts on shrub cover were large, but most pixels (61%) were projected to recover within 100 years (Figures S4 and S5).

Our first research question was, how long does it take for NPP and shrub cover in drylands to recover following a disturbance that removes all biomass and disrupts surface soil? We found that median recovery time for shrub cover was 81 years after the disturbance, with most sites (80%) projected to recover within 200 years after the initial disturbance. NPP recovery was projected to occur at 40% of sites within 20 years, but the majority of the remaining sites were not projected to recover within 200 years (Figure S4).

Our second research question asked, how do MAP, precipitation timing, and soil texture interact to influence recovery of NPP and shrub cover in drylands? Our results indicate that more precipitation does not drive rapid recovery. Rather, the initial impacts of disturbance and rate of recovery depend on soil texture, MAP, precipitation timing, and their interactions. In general, our results indicate that NPP recovery was fastest in cold and dry locations, and long-term recovery potential decreased in locations with coarse soils and warmer precipitation regimes (Figure 3). Shrub cover recovery was quickest on fine soils in warm precipitation regimes (Figure 4), but our field studies indicated that this recovery reflects the establishment and growth of different shrub species than those present in neighbouring undisturbed plots (Figure S6).

Both shrub cover and NPP values did not decline to zero following disturbance. This is likely due to several factors. First, we used annual NPP values, so depending on when the disturbance occurred, there is likely production prior to or in the period after the pipeline disturbance, but still within the year of the disturbance. Second, Landsat pixels do not always fit perfectly within pipeline allowing very small portions of undisturbed vegetation within each disturbed pixel. Third, though the remotely sensed estimates of NPP and shrub cover operate on reflectance, the algorithms were trained on large spatial datasets that may limit sensitivity to abrupt changes, and instead focus on predicting average landscape values to minimize error. Despite these factors we still observed moderate interannual variability in NPP and shrub cover both in disturbed pixels and in undisturbed pixels. We also observed that our model was able to capture various recovery trajectory shapes (Figures 3 and 4), such that it is unlikely that the lack of a strong initial disturbance impact would bias long term recovery trends.

Our results indicate that recovery of both productivity and shrub cover are generally enhanced by finer soil texture (Figures 3 and 4). This pattern persisted across gradients of MAP, indicating that the inverse texture hypothesis may not be easily applied to recovery and recruitment of dryland plants. However, soil texture interacted with precipitation regime to influence recovery of shrub cover (Figure 4; Table 1). Specifically, shrub recovery was similar on fine and coarse soil textures within cold precipitation regimes, but in warmer precipitation regimes shrub cover recovery was faster and more complete on fine-textured soils. This is opposite our prediction that coarse soils would benefit shrub cover recovery, especially in locations with low average precipitation and high evaporative losses that accompany warmer precipitation regimes. One explanation for this discrepancy could be tied to soil changes following pipeline construction. However, a review of pipeline construction effects on soil indicates that soil compaction, a very common phenomenon following pipeline installation, was most prevalent on fine-textured soils (Brehm & Culman, 2022). Therefore, soil manipulation tied to the pipeline disturbance is an unlikely mechanism to explain our observations of coarse soils being less favourable for recovery. Perhaps our results run counter to the inverse texture hypothesis because our study involves recruitment dynamics that respond to different factors than the dynamics of mature plants. Currently, there is no consensus in the literature regarding benefits of coarse soil for young plants (Barnard et al., 2019; Boyd & Davies, 2012; Lesica et al., 2007), in contrast to the consistent evidence for positive impacts of coarse soils on mature vegetation in dry environments (Renne et al., 2019).

4.1 | Contrasting shrub and NPP recovery

Areas that recovered shrub cover quickly did not recover NPP quickly, and vice versa (Figures 3 and 4). NPP recovery was concentrated in areas of cold precipitation regimes or very low NPP (Figure 3). We hypothesize that cold precipitation regimes favour NPP recovery due to high growth of forbs and grasses following disturbance. Our field surveys support these findings, with disturbed pipeline corridors in a cold precipitation regime having on average 2.5-fold more forbs and grasses than neighbouring undisturbed vegetation (10 years after disturbance). However, we observed little to no grasses or forbs in the disturbed pipeline corridors in the warmer Mojave Desert (30 years after disturbance), a system that sees periodic bursts of annual grasses and forbs during above-average water years. High grass cover has been shown to limit shrub recruitment (Davidson et al., 2019; Germino et al., 2018), particularly in cold precipitation regimes (Bates & Davies, 2022), which may explain the quick recovery of NPP and slower shrub cover recovery. However, in warm precipitation regimes, disturbance linked with soil disruption and erosion has been hypothesized to promote a shrub stable state (Okin et al., 2009; Schlesinger et al., 1990).

Invasive annual grasses may be influencing post-disturbance NPP recovery. Dominance of exotic annual grasses is generally linked to disturbance by fire (Fusco et al., 2019) and can alter the productivity of shrubland ecosystems (Nagy et al., 2021). Plant communities with low pre-disturbance NPP and cold precipitation regimes that showed the quickest NPP recovery in our study are also thought to be most susceptible to annual grass invasion (Chambers et al., 2014). Although our results do not specifically monitor for exotic annual grass abundance, we speculate that invasion by exotic annual grasses may, in-part, be contributing to the patterns of NPP recovery. We encourage further investigation regarding how invasion dynamics influence recovery of NPP following disturbance.

Our model predicts incomplete NPP recovery across many sites (58%), including those that had full shrub cover recovery (Figure S5). We hypothesize that this mismatch is tied to changes in species composition. In cold precipitation regimes, our field observations indicate that the same shrub species occur on disturbed and undisturbed sites (*Artemisia tridentata*, *Sarcobatus* spp., *Atriplex* spp.), whereas in warmer precipitation regimes, recovery of the dominant undisturbed shrub (usually *Larrea tridentata* or *Prosopis* spp.) was limited (Figure S6). In place of dominant shrubs such as *Larrea* spp., disturbed plant communities in warmer precipitation regimes consisted of small early successional species such as *Gutierrezia sarothrae*, *Ambrosia dumosa*, and small grass species. Many of these early successional species are known to reduce above-ground forage and production of plant communities due to competitive effects on other species, especially during years with below average precipitation (Nagy et al., 2021). This supports the findings of a review on disturbance in drylands showing that despite recovery of herbaceous cover, plant species composition often shifts to a new stable state following disturbance (Abella et al., 2021).

4.2 | Relative-recovery hypothesis

We hypothesized that time to recovery would either increase with higher water availability, or that high water availability would be associated with high undisturbed levels of production or shrub cover that would recover more slowly. We found that despite more production and shrub cover following disturbance, areas with high undisturbed levels of shrub cover and/or NPP did not return to undisturbed levels more quickly than areas with low undisturbed levels (Figure 5). We observed that some areas with very low undisturbed NPP appear to slightly increase in production following disturbance (Figure 5). This pattern supports a relative-recovery framework, where time to full recovery may be slower in resource rich locations despite faster year-to-year increases in shrub cover or NPP following disturbance.

Land use history is an important factor to consider in the relative-recovery framework. Arid locations with low undisturbed values

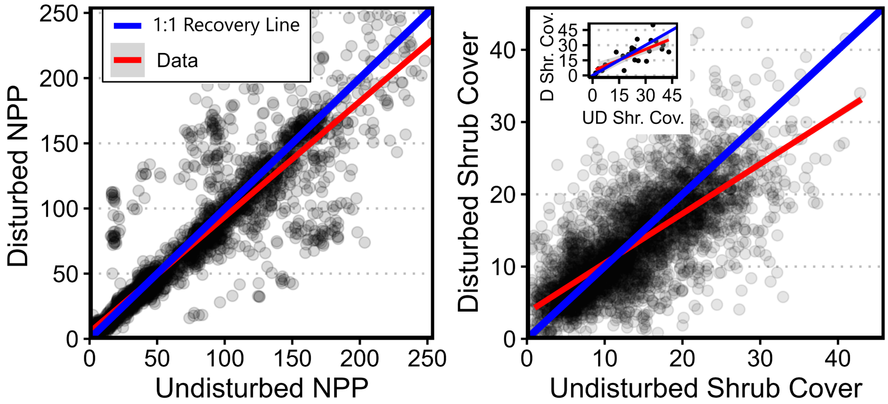

FIGURE 5 Plots comparing levels of net primary production (NPP; left) and total shrub cover (right) at disturbed locations with respect to their respective undisturbed control levels (*x* axis) 50–55 years after disturbance. Grey dots represent individual sites. The blue line represents recovery, where levels of a variable in a disturbed location return to the level of their undisturbed control. The red line represents a regression line for the dots/sites. Both plots use remotely sensed estimates of pixels disturbed 50–55 years after pipeline construction. The inset graph in the right panel uses field observations of total shrub cover at sites disturbed 61 and 75 years ago. All red regression lines are surrounded by a grey confidence interval representing standard error of the estimated slope; the high power of our large dataset results in narrow confidence intervals which are difficult to see.

of NPP and shrub cover may be more likely to be degraded than more productive systems due to historic livestock grazing (Hoover et al., 2020). These systems may recover quickly, but to a degraded or early successional state rather than to a later successional state. This emphasizes the importance of understanding pre-disturbance conditions, especially if they vary systematically across space with climate and land-use. Our analysis used undisturbed vegetation as a reference, but assessing the condition of the reference pixels was beyond the scope of our study.

Drylands are complex systems that are sensitive to physical disturbance (Svejcar & Kildisheva, 2017). Areas with high production tend to have more plant species and more diverse soil microbes (Adler & Levine, 2007; Maestre et al., 2015). Our results indicate that the complex biotic interactions that support high NPP and shrub cover within water-limited systems may require more time to reestablish following disturbance. Differential response of low and high productivity areas to disturbance may also be linked to changes in abundance of invasive annual grasses often associated with disturbance (D'Antonio & Vitousek, 1992), which can potentially lead to a higher ephemeral production in dry areas (Wolkovich et al., 2010). Our results may also indicate that post-disturbance recovery is slow or incomplete in locations where woody plants that utilize deep soil moisture are replaced with herbaceous vegetation or more shallow-rooted shrub species that cannot access deep soil water, resulting in a novel resource limitation on production. The notion that deep soil water may be out of reach of early successional plants is consistent with the relatively negative effect of coarse soils on recovery that we observed (Figures 3 and 4).

Given our results and estimates of recovery timelines, we recommend prioritizing the conservation of productive dryland plant communities that are unlikely to return to prior levels of function and composition, analogous to biodiversity hotspots in conservation biology.

AUTHOR CONTRIBUTIONS

Peter B. Adler secured funding, identified the general research questions, helped perform the analysis and provided extensive edits on manuscript. Tyson J. Terry identified hypotheses, collected and analysed the data and wrote the manuscript.

ACKNOWLEDGEMENTS

We would like to thank the editors, Sasha Reed, Bill Smith, Scott Ferrenberg, Osvaldo Sala, Brooke Osborne, Steven Lee, Sam Jordan and the anonymous reviewers for their feedback and ideas that strengthened this project. This project was funded by the United States Department of Defense Strategic Environmental Research and Development Program grant 201940 and Utah State University Graduate Research Award A07339-1068. All fieldwork was done on public lands with no destructive harvesting such that no fieldwork permits were required. Open Access funding enabled and organized by Projekt DEAL.

CONFLICT OF INTEREST STATEMENT

The authors have no conflicts of interest to report.

PEER REVIEW

The peer review history for this article is available at https://www.webofscience.com/api/gateway/wos/peer-review/10.1111/1365-2745.14306.

DATA AVAILABILITY STATEMENT

The data and R code to reproduce the analyses and figures used within this study are archived at Open Science Framework and publicly available at https://doi.org/10.17605/osf.io/mc6ed (Terry, 2023).

ORCID

Tyson J. Terry https://orcid.org/0000-0002-1839-0671
Peter B. Adler https://orcid.org/0000-0002-4216-4009

REFERENCES

Abella, S. R., Gentilcore, D. M., & Chiquoine, L. P. (2021). Resilience and alternative stable states after desert wildfires. *Ecological Monographs*, *91*(1), 1–19. https://doi.org/10.1002/ecm.1432

Adler, P. B., & Levine, J. M. (2007). Contrasting relationships between precipitation and species richness in space and time. *Oikos*, *116*(2), 221–232. https://doi.org/10.1111/j.2006.0030-1299.15327.x

Allred, B. W., Bestelmeyer, B. T., Boyd, C. S., Brown, C., Davies, K. W., Duniway, M. C., Ellsworth, L. M., Erickson, T. A., Fuhlendorf, S. D., Griffiths, T. V., Jansen, V., Jones, M. O., Karl, J., Knight, A., Maestas, J. D., Maynard, J. J., McCord, S. E., Naugle, D. E., Starns, H. D., … Uden, D. R. (2021). Improving Landsat predictions of rangeland fractional cover with multitask learning and uncertainty. *Methods in Ecology and Evolution*, *12*(5), 841–849. https://doi.org/10.1111/2041-210X.13564

Allred, B. W., Smith, W. K., Twidwell, D., Haggerty, J. H., Running, S. W., Naugle, D. E., & Fuhlendorf, S. D. (2015). Ecosystem services lost to oil and gas in North America. *Science*, *348*(6233), 401–402. https://doi.org/10.1126/science.aaa4785

Avirmed, O., Lauenroth, W. K., Burke, I. C., & Mobley, M. L. (2015). Sagebrush steppe recovery on 30–90-year-old abandoned oil and gas wells. *Ecosphere*, *6*(7), art115. https://doi.org/10.1890/es14-00175.1

Barnard, D. M., Germino, M. J., Arkle, R. S., Bradford, J. B., Duniway, M. C., Pilliod, D. S., Pyke, D. A., Shriver, R. K., & Welty, J. L. (2019). Soil characteristics are associated with gradients of big sagebrush canopy structure after disturbance. *Ecosphere*, *10*(6), e02780. https://doi.org/10.1002/ecs2.2780

Bartels, S. F., Chen, H. Y. H., Wulder, M. A., & White, J. C. (2016). Trends in post-disturbance recovery rates of Canada's forests following wildfire and harvest. *Forest Ecology and Management*, *361*, 194–207. https://doi.org/10.1016/j.foreco.2015.11.015

Bates, D., Mächler, M., Bolker, B., & Walker, S. (2015). *Fitting linear mixed-effects models using lme4*. https://doi.org/10.18637/jss.v067.i01

Bates, J. D., & Davies, K. W. (2022). Early succession following prescribed fire in low sagebrush (*Artemisia arbuscula* var. *arbuscula*) steppe. *Western North American Naturalist*, *82*(1), 50–66. https://doi.org/10.3398/064.082.0105

Boyd, C. S., & Davies, K. W. (2012). Spatial variability in cost and success of revegetation in a wyoming big sagebrush community. *Environmental Management*, *50*(3), 441–450. https://doi.org/10.1007/s00267-012-9894-6

Bradford, J. B., Schlaepfer, D. R., Lauenroth, W. K., Palmquist, K. A., Chambers, J. C., Maestas, J. D., & Campbell, S. B. (2019). Climate-driven shifts in soil temperature and moisture regimes suggest opportunities to enhance assessments of dryland resilience and resistance. *Frontiers in Ecology and Evolution*, *7*, 1–16. https://doi.org/10.3389/fevo.2019.00358

Brehm, T., & Culman, S. (2022). Pipeline installation effects on soils and plants: A review and quantitative synthesis. *Agrosystems, Geosciences & Environment*, *5*(4), e20312. https://doi.org/10.1002/agg2.20312

Chambers, J. C., Allen, C. R., & Cushman, S. A. (2019). Operationalizing ecological resilience concepts for managing species and ecosystems at risk. *Frontiers in Ecology and Evolution*, *7*, 241. https://doi.org/10.3389/fevo.2019.00241

Chambers, J. C., Bradley, B. A., Brown, C. S., D'Antonio, C., Germino, M. J., Grace, J. B., Hardegree, S. P., Miller, R. F., & Pyke, D. A. (2014). Resilience to stress and disturbance, and resistance to *Bromus tectorum* L. invasion in cold desert shrublands of western North America. *Ecosystems*, *17*(2), 360–375. https://doi.org/10.1007/S10021-013-9725-5

Chambers, J. C., Maestas, J. D., Pyke, D. A., Boyd, C. S., Pellant, M., & Wuenschel, A. (2017). Using resilience and resistance concepts to manage persistent threats to sagebrush ecosystems and greater sage-grouse. *Rangeland Ecology and Management*, *70*(2), 149–164. https://doi.org/10.1016/j.rama.2016.08.005

Chapin, F. S., Torn, M. S., & Masaki, T. (1996). Principles of ecosystem sustainability. *American Naturalist*, *148*(6), 1016–1037.

Condon, L., Weisberg, P. J., & Chambers, J. C. (2011). Abiotic and biotic influences on Bromus tectorum invasion and Artemisia tridentata recovery after fire. *International Journal of Wildland Fire*, *20*(4), 597–604. https://doi.org/10.1071/WF09082

D'Antonio, C., & Vitousek, P. (1992). Biological invasions by exotic grasses, the grass/fire cycle, and global change. *Annual Review of Ecology and Systematics*, *23*(1), 63–87. https://doi.org/10.1146/annurev.es.23.110192.000431

Davidson, B. E., Germino, M. J., Richardson, B., & Barnard, D. M. (2019). Landscape and organismal factors affecting sagebrush-seedling transplant survival after megafire restoration. *Restoration Ecology*, *27*(5), 1008–1020. https://doi.org/10.1111/rec.12940

Díaz-Delgado, R., Lloret, F., & Pons, X. (2003). Influence of fire severity on plant regeneration by means of remote sensing imagery. *International Journal of Remote Sensing*, *24*(8), 1751–1763. https://doi.org/10.1080/01431160210144732

Farrell, H. L., & Fehmi, J. S. (2018). Seeding alters plant community trajectory: Impacts of seeding, grazing and trampling on semi-arid revegetation. *Applied Vegetation Science*, *21*(2), 240–249. https://doi.org/10.1111/avsc.12340

Fick, S. E., & Hijmans, R. J. (2017). WorldClim 2: New 1 km spatial resolution climate surfaces for global land areas. *International Journal of Climatology*, *37*(12), 4302–4315. https://doi.org/10.1002/joc.5086

Fusco, E. J., Finn, J. T., Balch, J. K., Nagy, R. C., & Bradley, B. A. (2019). Invasive grasses increase fire occurrence and frequency across US ecoregions. *Proceedings of the National Academy of Sciences of the United States of America*, *116*(47), 23594–23599. https://doi.org/10.1073/pnas.1908253116

Germino, M. J., Barnard, D. M., Davidson, B. E., Arkle, R. S., Pilliod, D. S., Fisk, M. R., & Applestein, C. (2018). Thresholds and hotspots for shrub restoration following a heterogeneous megafire. *Landscape Ecology*, *33*(7), 1177–1194. https://doi.org/10.1007/s10980-018-0662-8

Gorelick, N., Hancher, M., Dixon, M., Ilyushchenko, S., Thau, D., & Moore, R. (2017). Google earth engine: Planetary-scale geospatial analysis for everyone. *Remote Sensing of Environment*, *202*, 18–27. https://doi.org/10.1016/j.rse.2017.06.031

Hengl, T., Mendes de Jesus, J., Heuvelink, G. B. M., Ruiperez Gonzalez, M., Kilibarda, M., Blagotić, A., Shangguan, W., Wright, M. N., Geng, X., Bauer-Marschallinger, B., Guevara, M. A., Vargas, R., MacMillan, R. A., Batjes, N. H., Leenaars, J. G. B., Ribeiro, E., Wheeler, I., Mantel, S., & Kempen, B. (2017). SoilGrids250m: Global gridded soil information based on machine learning. *PLOS ONE*, *12*(2), e0169748. https://doi.org/10.1371/journal.pone.0169748

Hodgson, D., McDonald, J. L., & Hosken, D. J. (2015). What do you mean, 'resilient'? *Trends in Ecology & Evolution*, *30*(9), 503–506. https://doi.org/10.1016/j.tree.2015.06.010

Hoover, D. L., Bestelmeyer, B., Grimm, N. B., Huxman, T. E., Reed, S. C., Sala, O., Seastedt, T. R., Wilmer, H., & Ferrenberg, S. (2020). Traversing the wasteland: A framework for assessing ecological threats to drylands. *Bioscience*, *70*(1), 35–47.

Ingrisch, J., & Bahn, M. (2018). Towards a comparable quantification of resilience. *Trends in Ecology & Evolution*, *33*(4), 251–259. https://doi.org/10.1016/j.tree.2018.01.013

Isles, P. D. F. (2020). The misuse of ratios in ecological stoichiometry. *Ecology*, *101*(11), e03153. https://doi.org/10.1002/ecy.3153

Jones, M. O., Allred, B. W., Naugle, D. E., Maestas, J. D., Donnelly, P., Metz, L. J., Karl, J., Smith, R., Bestelmeyer, B., Boyd, C., Kerby, J. D., & McIver, J. D. (2018). Innovation in rangeland monitoring: Annual, 30 m, plant functional type percent cover maps for US rangelands, 1984–2017. *Ecosphere*, *9*(9), e02430. https://doi.org/10.1002/ecs2.2430

Jordan, S. E., Palmquist, K. A., Bradford, J. B., & Lauenroth, W. K. (2020). Soil water availability shapes species richness in mid-latitude shrub steppe plant communities. *Journal of Vegetation Science*, *31*(4), 646–657. https://doi.org/10.1111/jvs.12874

Lauenroth, W. K., & Bradford, J. B. (2012). Ecohydrology of dry regions of the United States: Water balance consequences of small precipitation events. *Ecohydrology*, *5*(1), 46–53. https://doi.org/10.1002/eco.195

Lesica, P., Cooper, S. V., & Kudray, G. (2007). Recovery of big sagebrush following fire in southwest Montana. *Rangeland Ecology & Management*, *60*(3), 261–269. https://doi.org/10.2111/1551-5028(2007)60[261:robsff]2.0.co;2

Loik, M. E., Breshears, D. D., Lauenroth, W. K., & Belnap, J. (2004). A multi-scale perspective of water pulses in dryland ecosystems: Climatology and ecohydrology of the western USA. *Oecologia*, *141*(2), 269–281. https://doi.org/10.1007/S00442-004-1570-Y

Maestre, F. T., Delgado-Baquerizo, M., Jeffries, T. C., Eldridge, D. J., Ochoa, V., Gozalo, B., Quero, J. L., Garcia-Gomez, M., Gallardo, A., Ulrich, W., Bowker, M. A., Arredondo, T., Barraza-Zepeda, C., Bran, D., Florentino, A., Gaitan, J., Gutierrez, J. R., Huber-Sannwald, E., Jankju, M., … Singh, B. K. (2015). Increasing aridity reduces soil microbial diversity and abundance in global drylands. *Proceedings of the National Academy of Sciences of the United States of America*, *112*(51), 15684–15689. https://doi.org/10.1073/pnas.1516684112

Maurer, G. E., Hallmark, A. J., Brown, R. F., Sala, O. E., & Collins, S. L. (2020). Sensitivity of primary production to precipitation across the United States. *Ecology Letters*, *23*(3), 527–536. https://doi.org/10.1111/ele.13455

Monroe, A. P., Nauman, T. W., Aldridge, C. L., O'Donnell, M. S., Duniway, M. C., Cade, B. S., Manier, D. J., & Anderson, P. J. (2022). Assessing vegetation recovery from energy development using a dynamic reference approach. *Ecology and Evolution*, *12*(2), e8508. https://doi.org/10.1002/ece3.8508

Nagy, R. C., Fusco, E. J., Balch, J. K., Finn, J. T., Mahood, A., Allen, J. M., & Bradley, B. A. (2021). A synthesis of the effects of cheatgrass invasion on US Great Basin carbon storage. *Journal of Applied Ecology*, *58*(2), 327–337. https://doi.org/10.1111/1365-2664.13770

Nelson, Z. J., Weisberg, P. J., & Kitchen, S. G. (2014). Influence of climate and environment on post-fire recovery of mountain big sagebrush. *International Journal of Wildland Fire*, *23*(1), 131–142. https://doi.org/10.1071/WF13012

Nimmo, D. G., Mac Nally, R., Cunningham, S. C., Haslem, A., & Bennett, A. F. (2015). Vive la résistance: Reviving resistance for 21st century conservation. *Trends in Ecology & Evolution*, *30*(9), 516–523. https://doi.org/10.1016/j.tree.2015.07.008

Noy-Meir, I. (1973). Desert ecosystems: Environment and producers. *Annual Review of Ecological Systems*, *24*(1), 25–51.

O'Brien, S. A., Dehling, D. M., & Tylianakis, J. M. (2022). The recovery of functional diversity with restoration. *Ecology*, *103*(3), e3618. https://doi.org/10.1002/ecy.3618

O'Connor, R. C., Germino, M. J., Barnard, D. M., Andrews, C. M., Bradford, J. B., Pilliod, D. S., Arkle, R. S., & Shriver, R. K. (2020). Small-scale water deficits after wildfires create long-lasting ecological impacts. *Environmental Research Letters*, *15*(4), 044001. https://doi.org/10.1088/1748-9326/ab79e4

Okin, G. S., D'Odorico, P., & Archer, S. R. (2009). Impact of feedbacks on Chihuahuan desert grasslands: Transience and metastability. *Journal of Geophysical Research*, *114*, 1004. https://doi.org/10.1029/2008JG000833

Oliver, T. H., Heard, M. S., Isaac, N. J. B., Roy, D. B., Procter, D., Eigenbrod, F., Freckleton, R., Hector, A., Orme, C. D. L., Petchey, O. L., Vânia, P., Raffaelli, D., Suttle, K. B., Mace, G. M., Matin-Lopez, B., Woodcock, B. A., & Bullock, J. M. (2015). Biodiversity and resilience of ecosystem functions. *Trends in Ecology & Evolution*, *30*(11), 673–684. https://doi.org/10.1016/j.tree.2015.08.009

Parker, K. R., & Wiens, J. A. (2005). Assessing recovery following environmental accidents: Environmental variation, ecological assumptions, and strategies. *Ecological Applications*, *15*(6), 2037–2051. https://doi.org/10.1890/04-1723

Peinado, M., Alcaraz, F., Aguirre, J. L., & Delgadillo, J. (1995). Major plant communities of warm North American deserts. *Journal of Vegetation Science*, *6*(1), 79–94. https://doi.org/10.2307/3236259

R Core Team. (2022). *R: A language and environment for statistical computing*. R Foundation for Statistical Computing. https://www.R-project.org/

Renne, R. R., Bradford, J. B., Burke, I. C., & Lauenroth, W. K. (2019). Soil texture and precipitation seasonality influence plant community structure in North American temperate shrub steppe. *Ecology*, *100*(11), e02824. https://doi.org/10.1002/ecy.2824

Robinson, N. P., Jones, M. O., Moreno, A., Erickson, T. A., Naugle, D. E., & Allred, B. W. (2019). Rangeland productivity partitioned to sub-pixel plant functional types. *Remote Sensing*, *11*, 1427. https://doi.org/10.3390/rs11121427

Rottler, C. M., Burke, I. C., Palmquist, K. A., Bradford, J. B., & Lauenroth, W. K. (2018). Current reclamation practices after oil and gas development do not speed up succession or plant community recovery in big sagebrush ecosystems in Wyoming. *Restoration Ecology*, *26*(1), 114–123. https://doi.org/10.1111/rec.12543

Sala, O. E., Gherardi, L. A., Reichmann, L., Jobbágy, E., & Peters, D. (2012). Legacies of precipitation fluctuations on primary production: Theory and data synthesis. *Philosophical Transactions of the Royal Society B*, *367*(1606), 3135–3144. https://doi.org/10.1098/rstb.2011.0347

Sala, O. E., Parton, W. J., Joyce, L. A., & Lauenroth, W. K. (1988). Primary production of the central grassland region of the United States. *Ecology*, *69*(1), 40–45. https://doi.org/10.2307/1943158

Schlesinger, W. H., Reynolds, J. F., Cunningham, G. L., Laura, F., Jarrell, W. M., Virginia, R. A., & Whitford, W. G. (1990). Biological feedbacks in global desertification conceptual models for desertification. *Science*, *247*(4946), 1043–1048.

Shi, P., Xiao, J., Wang, Y. F., & Chen, L. D. (2014). The effects of pipeline construction disturbance on soil properties and restoration cycle. *Environmental Monitoring and Assessment*, *186*, 1825–1835. https://doi.org/10.1007/s10661-013-3496-5

Shriver, R. K., Andrews, C. M., Pilliod, D. S., Arkle, R. S., Welty, J. L., Germino, M. J., Duniway, M. C., Pyke, D. A., & Bradford, J. B. (2018). Adapting management to a changing world: Warm temperatures, dry soil, and interannual variability limit restoration success of a dominant woody shrub in temperate drylands. *Global Change Biology*, *4*(10), 4972–4982. https://doi.org/10.1111/gcb.14374

Stafford Smith, D. M., Abel, N., Walker, B., & Chapin, F. S. (2009). Drylands: Coping with uncertainty, thresholds, and changes in state. In *Principles of ecosystem stewardship* (pp. 171–195). Springer. https://doi.org/10.1007/978-0-387-73033-2_8

Suring, L. H., Rowland, M. M., & Wisdom, M. J. (2005). Identifying species of concern. In M. J. Wisdom, M. M. Rowland, & L. H. Suring (Eds.), *Habitat threats in the sagebrush ecosystem—Methods of regional assessment and applications in the Great Basin* (pp. 150–162). Alliance Communications Group.

Svejcar, L. N., & Kildisheva, O. A. (2017). The age of restoration: Challenges presented by dryland systems. *Plant Ecology*, *218*(1), 1–6. https://doi.org/10.1007/s11258-016-0694-6

Terry, T. J. (2023). *Natural gas pipeline recovery data and analysis*. Open Science Framework. https://doi.org/10.17605/osf.io/mc6ed

Thornton, M., Shrestha, R., Wei, Y., Thornton, P., Kao, S., & Wilson, B. E. (2022). *Daymet: Daily surface weather data on a 1-km grid for North America, version 4*. ORNL DAAC.

Tilman, D. (2016). The resource-ratio hypothesis of plant succession. *American Naturalist*, *125*(6), 827–852.

Tomislav, H. (2018). Sand content in % (kg/kg) at 6 standard depths (0, 10, 30, 60, 100 and 200 cm) at 250 m resolution (v0.2). *Zenodo*. https://doi.org/10.5281/zenodo.2525662

USDOT. (2021). *United States Department of Transportation National Pipeline Mapping System*. https://pvnpms.phmsa.dot.gov/PublicViewer

Walter, H. (1964). *Vegetation der Erde in oko-physiologischer Betrachtung*. Gustav Fischer.

Wessels, K. J., Prince, S. D., & Reshef, I. (2008). Mapping land degradation by comparison of vegetation production to spatially derived estimates of potential production. *Journal of Arid Environments*, *72*(10), 1940–1949. https://doi.org/10.1016/j.jaridenv.2008.05.011

Wolkovich, E. M., Lipson, D. A., Virginia, R. A., Cottingham, K. L., & Bolger, D. T. (2010). Grass invasion causes rapid increases in ecosystem carbon and nitrogen storage in a semiarid shrubland. *Global Change Biology*, *16*(4), 1351–1365. https://doi.org/10.1111/j.1365-2486.2009.02001.x

Zhu, J., & Morgan, G. D. (2004). Comparison of spatial variables over subregions using a block bootstrap. *Journal of Agricultural, Biological, and Environmental Statistics*, *9*(1), 91–104. https://doi.org/10.1198/1085711043154

Zika, M., & Erb, K. H. (2009). The global loss of net primary production resulting from human-induced soil degradation in drylands. *Ecological Economics*, *69*(2), 310–318. https://doi.org/10.1016/j.ecolecon.2009.06.014

SUPPORTING INFORMATION

Additional supporting information can be found online in the Supporting Information section at the end of this article.

Figure S1. Diagnostic plots of shrub cover model. Residuals versus fitted values (left) and histogram (right).

Figure S2. Diagnostic plots of net primary production model.

Figure S3. Map indicating the spatial extent of three precipitation regimes in North American Deserts: areas that receive the majority of their precipitation in cold temperatures, areas that receive the majority of their precipitation in the cool temperatures and those that receive the majority of their precipitation in warm temperatures.

Figure S4. Modelled recovery dynamics of all pixels within study.

Figure S5. Estimated recovery timing of shrub cover (left) and net primary production (right).

Figure S6. Recovery ratio values (shrub cover in disturbed plots/shrub cover in undisturbed control plots) of the dominant shrub species in undisturbed conditions across our field observations.

Figure S7. Location of field sites (circles) along pipelines (lines).

How to cite this article: Terry, T. J., & Adler, P. B. (2024). Precipitation seasonality and soil texture interact to shape dryland recovery from severe disturbance. *Journal of Ecology*, *112*, 1356–1368. https://doi.org/10.1111/1365-2745.14306